Multi-User Analog Beamforming in mmWave MIMO Systems Based on Path Angle Information

Lisi Jiang and Hamid Jafarkhani

Abstract

We aim to design an analog-only beamforming scheme for downlink multi-user mmWave systems to optimize the beamforming gain and the inter-user interference at the same time. Traditional analog beamforming scheme, such as beam selection method, uses the array response vector corresponding to the strongest path of the channel to generate a beam pointing to the user. In multi-user systems, such schemes will lead to large inter-user interference, especially when the users are located closely. In this paper, we formulate a multi-objective problem to strike a balance between the beamforming gain and the inter-user interference. To solve the problem, we first use the weighted-sum method to transform the multi-objective problem into a single-objective problem. Then, we use the semi-definite programing technique to make the analog beamforming with constant-magnitude constraints tractable. Furthermore, to alleviate the effects of the channel estimation and feedback quantization errors, we design a robust beamforming scheme to provide robustness against imperfect channel information. We first develop a channel error model for the scattering clustered channel model, which can serve as a general channel error model for mmWave channels. Then, we formulate a multi-objective problem using the stochastic approach to suppresse the interference and enhance the beamforming gain at the same time. Simulation results show that our proposed non-robust multi-user analog beamformer outperforms the traditional analog beamforming method when SNR is high and our proposed robust beamformer can provide up to 109% improvement in the sum-rate compared to the beam selection method.

I. Introduction

Millimeter wave (mmWave) communication has been considered as a key technology for future wireless communication systems because of the high data rates provided by the large bandwidths at mmWave carrier frequencies. However, mmWave carrier frequencies suffer from

The authors are with the Center for Pervasive Communications and Computing, University of California at Irvine, Irvine, CA 92697, USA (email: {lisi.jiang, hamidj}@uci.edu). This work was supported in part by the NSF Award ECCS-1642536.

relatively severe propagation losses, which reduce service coverage and impair communication performance [1]. Thus, large antenna arrays are usually proposed to be implemented at both transmitters and receivers to provide sufficient beamforming gain to mitigate the severe propagation attenuation [2], [3]. The large antenna arrays, however, lead to high system complexity for employing conventional full digital beamforming, where each antenna element is connected to a separate radio-frequency (RF) chain [4]–[6]. Therefore, analog beamforming [7]–[9], where a single RF chain is tied to the entire antenna array and the beamforming processing is performed with the RF analog components, has been reignited in mmWave systems. To strike a balance between the system complexity and the beamforming precision, a hybrid architecture [10] that uses analog phase shifters in conjunction with a reduced number of RF chains is proposed for single-user mmWave multi-input multi-output (MIMO) systems.

To further improve the system throughput, multi-user systems, where a base station (BS) simultaneously serves a number of mobile stations, are often adopted. To cancel the interference among mobile stations, precoding is usually applied at the BS. For conventional multi-user systems, precoding is commonly done at the baseband, where each antenna element has a radio frequency (RF) chain [4], [11]–[17]. This kind of precoding is called fully digital beamforming. In [11], [12], [15], iterative beamforming algorithms that maximize the signal-to-interference-noise ratio (SINR) for all users were proposed. Unfortunately, these exists no closed-form solution for such iterative algorithms. Besides, the optimization problem is NP-complete, which means that they cannot be solved in reasonable time [16]. In [4] and [17], zero-forcing schemes for multi-user beamforming were proposed, which decoupled the multi-user beamforming problem and perfectly cancel the interference. In [13], [14], [16], the signal-to-leakage-and-noise ratio (SLNR) was chosen as the criterion of the optimization problem, which also leads to a decoupled optimization problem and provides an analytical closed-form solution. Also, in [16], a semidefinite-programming-based algorithm was proposed, which aims to minimize the total transmitted power with QoS requirements. However, similar to the single-user MIMO systems, all mentioned fully digital beamforming schemes are not practical for large antenna arrays in mmWave systems due to the high complexity and the large power consumption.

To address the difficulty of the limited number of RF chains in multi-user systems, two approaches have been proposed. One is the hybrid multi-user beamforming, in which the beamformer is constructed by the concatenation of a low-dimensional baseband (digital) beamformer and an RF (analog) beamformer [18]–[20]. The RF beamformer provides a high-dimensional phase-only control and is usually used to enhance the array gain. The baseband beamformer, on the other hand, is usually used to cancel the interference. This method can achieve a performance close to a conventional digital beamformer [18], [19]. However, a two-stage feedback for both the RF beamforming and the baseband beamforming is needed. Such a two-stage feedback requires a tremendous overhead for large antenna arrays. This may become a limitation for mmWave MIMO systems and should be avoided if possible. The other approach is the analog multi-user beamforming, where the beamforming processing is only performed with RF analog components. Currently, many RF beamformers use discrete Fourier transform (DFT) vectors as the RF beamformer [21]–[23]. Since the DFT vectors have a form similar to that of the array response vectors of the arrays, such an RF beamformer will have the largest array gain [19], [21]. Additionally, in [24]–[26], an analog beam selection method for mmWave multi-user systems was proposed, where both the BS and the users are equipped with an analog beamforming codebook. The codebook consists of beamforming vectors which are the array response vectors with uniform spacing. The BS chooses the best beamforming vector, which maximizes the beamforming gain, from the codebook. This method performs well for line-of-sight (LOS) channels, because the selected beamformer is the match filters for the LOS channels. However, considering a non-LOS (NLOS) channel model, the performance of the beam selection method will be degraded due to the interference among different paths and different users. Besides, the beam selection method needs a training stage to find the best beam, whose overhead scales linearly with the number of users. All of the previous work either uses DFT vectors as the analog beamformers or uses the array response vectors as the analog beamformers. To the best of our knowledge, there is no structure design for the analog beams in the literature.

In this paper, we aim to design an analog beamforming method in downlink multi-user systems which not only enhances the beamforming gain but also cancels the inter-user interference. In our method, the analog beams are not DFT structured vectors, but the objectives to be optimized. In the first part of the paper, we propose an analog beamforming method based on perfect channel state information (CSI). A multi-objective problem (MOP) is first established to maximize the beamforming gain and minimize the inter-user interference at the same time. We transform the MOP into a single-objective problem (SOP) by using the weighted-sum method. The semi-definite programming (SDP) technique is then introduced to deal with the constant-magnitude constraints for the analog beamforming. To further reduce the feedback overhead, we only use the angle of departures/angle of arrivals (AoD/AoA) of the channel instead of the full channel information.

Channel information is also critical for mmWave MIMO systems. Imperfect CSI will lead to severe performance degradation. Some papers, such as [27], [28] and [29], analyzed the performance of the imperfect CSI and proposed communication schemes for imperfect CSI in traditional MIMO systems, i.e., fully digital MIMO systems. However, to the best of our knowledge, there is no robust communication design for mmWave MIMO systems in the literature.

The second part of the paper considers imperfect CSI caused by channel estimation and quantization in mmWave systems. We propose a robust design for the analog beamforming, which not only suppresses the interference and enhances the beamforming gain, but also provides robustness against imperfect CSI. We assume there exists angle errors in the AoD/AoA of the channel and simplify the error model into an additive error model by using Taylor expansion. Based on the statistical properties of the errors, a probabilistic objective similar to [30]–[32] is formulated. We maximize the average beamforming gain while keeping the probability of small leakage power as large as possible (i.e., we formulate a MOP to maximize the average array gain and the probability of small leakage power at the same time). The probabilistic objective is transformed into a deterministic one by applying Markov's inequality, and then we use the same technique as the proposed non-robust beamforming to deal with the MOP for robust beamforming.

The contributions of our paper can be summarized as follows:

- We propose an analog beamforming scheme based on the path angle information in mmWave systems. The scheme strikes a balance between beamforming gain and inter-user interference only using partial channel information. Our proposed scheme outperforms the conventional beam selection method due to the interference suppression.
- We consider the effects of the channel estimation and feedback quantization errors and develop a channel error model for the scattering clustered channel model, which can serve as a general channel error model for mmWave channels.
- We propose a robust analog beamforming scheme for mmWave systems to alleviate the effects of the channel estimation and feedback quantization errors. The proposed robust analog beamforming scheme brings about 109% improvement in sum-rate compared to the conventional beam selection method.

The remaining sections are organized as follows. In Section II , we describe the system model and the mmWave channel model. Section III formulates the proposed analog beamforming

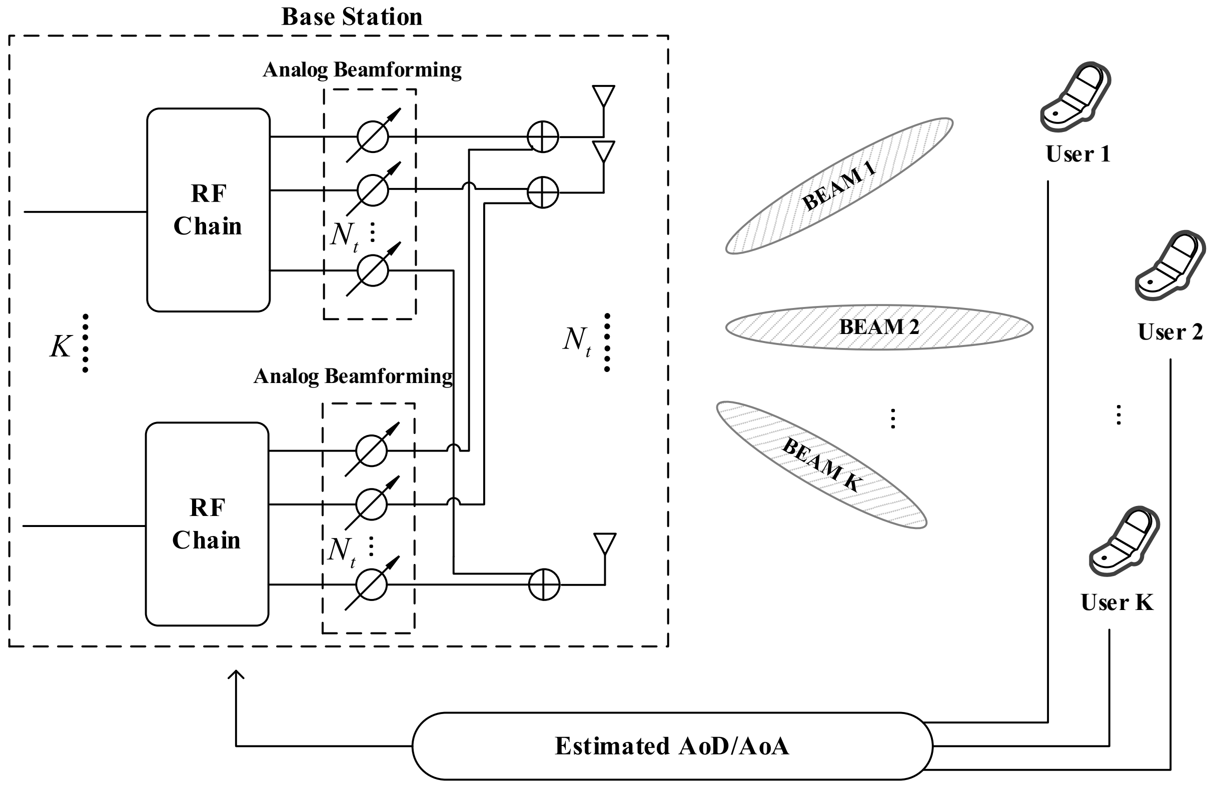

Fig. 1: System model

method based on perfect CSI. Section IV presents the proposed robust analog beamforming design for imperfect CSI. Numerical examples are presented and discussed in Section V. We provide concluding remarks in Section VI.

Notation: $\mathbb{C}^{m\times n}$ is the set of all $m\times n$ complex matrices with $\mathbb{C}^m \triangleq \mathbb{C}^{m\times 1}$ and $\mathbb{C} \triangleq \mathbb{C}^1$. $\mathbb{I}_m$ is the $m\times m$ identity matrix, and $\mathbf{0}_{m\times n}$ is the $m\times n$ all-zero matrix. $\mathcal{CN}(\boldsymbol{\mu},\mathbf{K})$ is a circularly-symmetric complex Gaussian random vector with mean vector $\boldsymbol{\mu}$ and covariance matrix $\mathbf{K}$. Matrices $\mathbf{A}^T$ and $\mathbf{A}^H$ are the transpose and the Hermite transpose of matrix $\mathbf{A}$, respectively. Matrix $\mathbf{A} = [\boldsymbol{\alpha}_1, \boldsymbol{\alpha}_2, ..., \boldsymbol{\alpha}_L]$ represents the concatenation of the L vectors $\boldsymbol{\alpha}_i$, and $\mathbf{B} = [\mathbf{A}_1, \mathbf{A}_2, ..., \mathbf{A}_K]$ represents the concatenation of the K matrices $\mathbf{A}_i$.

II. System model and problem formulation

A. System model and zero-forcing schemes

We consider a multi-user system including a BS with N_t antennas serving K single-antenna users as Fig. 1 depicts. The number of RF chains N_{RF} is set to be K to enable the multi-user transmission. In the case that the number of RF chains, N_{RF}, is less than the number of users, one can select N_{RF} out of K users and serve them using our algorithm. One such a user selection method is the proportional-fair (PF) method presented in [33]. Only analog beamforming is used for each user. The BS generates the analog beamforming vector for User i based on the estimated multi-path angles of the channels. We denote s_i as the transmitted symbol intended for User i with $E[\|s_i\|^2] = 1$ and $\boldsymbol{w}_i \in \mathbb{C}^{N_t \times 1}$ as the beamforming vector for s_i. The channel between User i and the BS is denoted by $\boldsymbol{h}_i^H \in \mathbb{C}^{1 \times N_t}$. The received signal at User i can be expressed as

$$y_i = \boldsymbol{h}_i^H \boldsymbol{w}_i s_i + \sum_{k=1, k \neq i}^{K} \boldsymbol{h}_i^H \boldsymbol{w}_k s_k + n_i, \tag{1}$$

where n_i is the additive Gaussian noise with zero mean and σ^2 variance. The second term in (1) is called the co-channel interference (CCI) caused by other users.

Intuitively, the optimal multi-user system is the one that maximizes the signal-to-interference-plus-noise ratio (SINR) of every user. The SINR of User i is given by

$$SINR_i = \frac{|\boldsymbol{h}_i^H \boldsymbol{w}_i|^2}{\sigma^2 + \sum_{k=1, k \neq i}^{K} |\boldsymbol{h}_i^H \boldsymbol{w}_k|^2}. \tag{2}$$

However, using SINR as the optimization criterion generally results in a challenging optimization problem to deal with K coupled variables $\{\boldsymbol{w}_i\}_{i=1}^K$ [11], [12], [15].

One way to avoid solving the coupled problem is to focus on canceling the CCI by using zero-forcing (ZF) schemes [34]. As [4] and [17] did, the ZF schemes choose beamforming vectors $\boldsymbol{w}_i$ by enforcing the conditions

$$\boldsymbol{h}_k^H \boldsymbol{w}_i = 0, \ \forall i, \ k = 1, ..., K, k \neq i. \tag{3}$$

This solution results in good performance since it completely cancels the CCI at every receiver. However, ZF does not optimize the beamforming gain, and thus is not optimal for SINR. Moreover, for analog beamforming, the elements of vector $\boldsymbol{w}_i$ have constant magnitudes, i.e., $|w_i^n| = constant$ where w_i^n denotes the n^{th} element in vector $\boldsymbol{w}_i$. We call these constraints, the constant-magnitude constraints. For a system with constant-magnitude constraints, the ZF conditions in (3) may not be feasible. To remedy these issues, we relax the ZF conditions in (3) and take the beamforming gain into account when choosing $\boldsymbol{w}_i$. The details will be explained in subsequent sections. In the next section, we will introduce the mmWave channel model which is very different from the traditional Rayleigh fading channel model. Based on the mmWave channel model, we will formulate our analog multi-user beamforming problem for mmWave systems.

B. Channel model

MmWave channels are expected to have limited scattering characteristic [35], which means the assumptions of a rich scattering environment become invalid. This is called sparsity in the literature and leads to the unreliability of traditional channel models, such as the Rayleigh fading channel model. To characterize the limited scattering feature, we adopt the clustered mmWave channel model in [10] and [36] with L_i scatters for the channel of User i. Each scatter is assumed to contribute a single propagation path between the BS and the user. For our single-antenna user system, the channel is modeled as a vector described by

$$\boldsymbol{h}_i^H = \sqrt{\frac{N_t}{L_i}} \sum_{l=1}^{L_i} (a_l^i)^* \boldsymbol{\alpha}_t(\theta_l^i)^H, \tag{4}$$

where $\boldsymbol{\alpha}_t(\theta_l^i)$ is the antenna array response vectors of the BS for path l with departure angle θ_l^i. Parameter $(a_l^i)^*$ is the complex path gain of path l modeled by a complex Gaussian distribution such as $\mathcal{CN}(0,1)$. While the algorithms and results in the paper can be applied to arbitrary antenna arrays, we use uniform linear arrays (ULAs) in the simulations for simplicity. The array response vectors take the following form

$$\boldsymbol{\alpha}_t(\theta_l^i) = \frac{1}{\sqrt{N_t}}[1, e^{j\frac{2\pi}{\lambda}d\sin(\theta_l^i)}, ..., e^{j(N_t-1)\frac{2\pi}{\lambda}d\sin(\theta_l^i)}], \tag{5}$$

where λ is the signal wavelength, and d is the distance between antenna elements. The departure angle θ_l^i is assumed to have a uniform distribution over $[0, 2\pi]$.

To simplify the expression of the channels, we denote

$$\mathbf{A}_i = [\boldsymbol{\alpha}_t(\theta_1^i), \boldsymbol{\alpha}_t(\theta_2^i), ..., \boldsymbol{\alpha}_t(\theta_L^i)], \tag{6}$$

$$\tilde{\boldsymbol{h}}_i = [a_1^i, a_2^i, ..., a_L^i]^T. \tag{7}$$

Matrix $\mathbf{A}_i \in \mathbb{C}^{N_t \times L_i}$ contains all the array response vectors from the BS to User i and vector $\tilde{\boldsymbol{h}}_i \in \mathbb{C}^{L_i \times 1}$ contains the complex gain of all the paths from the BS to User i. The channel $\boldsymbol{h}_i^H$ can be expressed as the product of Hermitian $\tilde{\boldsymbol{h}}_i$ and Hermitian $\mathbf{A}_i$

$$\boldsymbol{h}_i^H = \tilde{\boldsymbol{h}}_i^H \mathbf{A}_i^H. \tag{8}$$

We call $\mathbf{A}_i$ the AoD matrix of User i. In fact, to estimate the mmWave channels is to estimate the AoDs and the complex gains. In this paper, to further reduce the feedback overhead, we assume the BS only knows the AoD of the channels (i.e., the BS only knows $\mathbf{A}_i$).

C. Problem formulation

As we mentioned in the previous section, ZF schemes may not be effective for multi-user analog beamforming since the constant-magnitude constraints on $\boldsymbol{w}_i$ may cause the ZF conditions in (3) infeasible. To deal with this problem, we relax the equality condition in (3) and try to minimize the leakage interference. To be specific, we denote the leakage interference matrix as

$$\tilde{\mathbf{I}}_i = [\mathbf{A}_1, ..., \mathbf{A}_{i-1}, \mathbf{A}_{i+1}, ..., \mathbf{A}_K]^H, \tag{9}$$

where $\tilde{\mathbf{I}}_i \in \mathbb{C}^{\sum_{k=1,k\neq i}^{K} L_k \times N_t}$ is a matrix that contains the AoD matrices from the BS to all the users except User i. Originally, $\tilde{\mathbf{I}}_i$ should contain the channel vectors from the BS to all the users except User i. Since we assume we only know the AoDs of the channels, we use AoD matrices to represent the channels.

The traditional ZF schemes are basically forcing the $\boldsymbol{w}_i$ to lie in the null space of $\tilde{\mathbf{I}}_i$ so as to avoid the interference from User i to other users. The null space of $\tilde{\mathbf{I}}_i$ can be obtained through singular-value decomposition (SVD). We define the SVD of $\tilde{\mathbf{I}}_i$ as

$$\tilde{\mathbf{I}}_i = \tilde{\mathbf{U}}_i \tilde{\Sigma}_i [\tilde{\mathbf{V}}_i^{(1)} \quad \tilde{\mathbf{V}}_i^{(0)}]^H, \tag{10}$$

where $\tilde{\mathbf{V}}_i^{(1)}$ holds the first $\sum_{k=1,k\neq i}^{K} L_k$ right singular vectors and $\tilde{\mathbf{V}}_i^{(0)}$ holds the last $N_t - \sum_{k=1,k\neq i}^{K} L_k$ right singular vectors. We assume that we implement a large antenna array at the BS, which means N_t is very large. Note that the mmWave channels have limited scattering characteristic, which means L_k is usually small. Normally, $N_t \gg L_k$. Therefore, we assume $N_t > \sum_{k=1,k\neq i}^{K} L_k$ to ensure that the null space of $\tilde{\mathbf{I}}_i$ (i.e., $\tilde{\mathbf{V}}_i^{(0)}$) exists.

For the multi-user analog beamforming, where ZF conditions may be infeasible, we want to minimize the leakage interference of $\boldsymbol{w}_i$. That is actually minimizing the projection from $\boldsymbol{w}_i$ to $\tilde{\mathbf{I}}_i$, which means $\boldsymbol{w}_i$ should have the largest projection on the null space of $\tilde{\mathbf{I}}_i$. In other words, we are trying to find the $\boldsymbol{w}_i$ that has the largest projection on the null space of $\tilde{\mathbf{I}}_i$. The projected vector from $\boldsymbol{w}_i$ to the null space of $\tilde{\mathbf{I}}_i$ is

$$\boldsymbol{w}_i^p = \tilde{\mathbf{V}}_i^{(0)} (\tilde{\mathbf{V}}_i^{(0)})^H \boldsymbol{w}_i, \tag{11}$$

where $\tilde{\mathbf{V}}_i^{(0)}(\tilde{\mathbf{V}}_i^{(0)})^H$ is the projector matrix onto the the null space of $\tilde{\mathbf{I}}_i$. For simplicity, we maximize the square of the norm of $\boldsymbol{w}_i^p$ which is

$$\|\boldsymbol{w}_i^p\|^2 = \boldsymbol{w}_i^H \tilde{\mathbf{V}}_i^{(0)}(\tilde{\mathbf{V}}_i^{(0)})^H \tilde{\mathbf{V}}_i^{(0)}(\tilde{\mathbf{V}}_i^{(0)})^H \boldsymbol{w}_i = \boldsymbol{w}_i^H \tilde{\mathbf{V}}_i^{(0)}(\tilde{\mathbf{V}}_i^{(0)})^H \boldsymbol{w}_i. \tag{12}$$

To obtain an optimal SINR, only to minimize the leakage interference is not enough, since it ignores the beamforming gain. The beamforming gain refers to the improvement of the receive power which results from beamforming and we define the beamforming gain for $\boldsymbol{w}_i$ under our partial channel information assumption as

$$BG = \boldsymbol{w}_i^H \mathbf{A}_i \mathbf{A}_i^H \boldsymbol{w}_i. \tag{13}$$

Taking both the beamforming gain and the leakage interference into account, we formulate a multi-objective optimization problem (MOP) as follows:

$$\begin{aligned} \boldsymbol{w}_i^{opt} &= \operatorname{argmax}\{\boldsymbol{w}_i^H \tilde{\mathbf{V}}_i^{(0)}(\tilde{\mathbf{V}}_i^{(0)})^H \boldsymbol{w}_i, \boldsymbol{w}_i^H \mathbf{A}_i \mathbf{A}_i^H \boldsymbol{w}_i\} \\ s.t. \quad & \boldsymbol{w}_i \in \mathcal{W}, \end{aligned} \tag{14}$$

where $\mathcal{W}$ is the set of all constant-magnitude vectors with each element having a magnitude of $\frac{1}{\sqrt{N_t}}$. Problem (14) is a multi-objective problem with non-convex constraints, which is intractable. In the next section, we will solve this problem by the weighted sum method and the SDP technique.

III. Multi-user analog beamforming

To solve Problem (14), we are actually facing two challenges: 1) how to deal with the multi-objective problem; and 2) how to handle the non-convex constraints. For the MOP, we will use the simplest yet effective method (i.e., the weighted sum method), to transform it into an SOP. Then, through some algebraic transformation, we will transform the non-convex problem into an SDP and solve it using convex optimization.

A. Transforming the MOP into an SOP

The solution to an MOP may not exist because a single point that optimizes all objectives simultaneously usually does not exist. The idea of Pareto optimality is usually used to describe solutions for MOPs. A solution point is Pareto optimal if it is not possible to move from that point and improve at least one objective function without detriment to any other objective function.

Alternatively, a point is weakly Pareto optimal if it is not possible to move from that point and improve all objective functions simultaneously. To solve an MOP, we need to ensure the necessary and/or sufficient condition for Pareto optimality. In other words, to solve an MOP is to find the Pareto optimal points. There are many ways to find the Pareto optimal points. Two general methods are visualization and scalarization. A scalarization method specifies a goal function $f : R^M \to R$ that for any conceivable operating point, it produces a scalar describing how preferable that point is (large value means high preference). To be specific, it means to solve the optimization problem:

$$\begin{aligned} &\max_{\boldsymbol{x}} f(g_1(\boldsymbol{x}), ..., g_M(\boldsymbol{x})) \\ s.t. \quad &\boldsymbol{x} \in \mathcal{X} \end{aligned} \tag{15}$$

where $g_i(\boldsymbol{x})$ is the i^{th} objective function in the original MOP and $\mathcal{X}$ is the feasible region. For the weighted-sum method, function f is a weighted summation of the objective functions. As stated in [37], the weighted sum method can provide a sufficient condition for Pareto optimality if all the weights are positive and the summation of the weights is equal to one. In other words, the solution to the SOP formulated by the weighted summation is Pareto optimal for the MOP.

Applying the weighted sum method to our problem results in

$$\begin{aligned} &\boldsymbol{w}_i^{opt} = \text{argmax}\{\lambda_1 \boldsymbol{w}_i^H \tilde{\mathbf{V}}_i^{(0)} (\tilde{\mathbf{V}}_i^{(0)})^H \boldsymbol{w}_i + \lambda_2 \boldsymbol{w}_i^H \mathbf{A}_i \mathbf{A}_i^H \boldsymbol{w}_i\} \\ s.t. \quad &\boldsymbol{w}_i \in \mathcal{W} \end{aligned} \tag{16}$$

where $\lambda_1 + \lambda_2 = 1$ and $\lambda_i > 0, i \in \{1,2\}$. Parameter λ_i represents the importance of the i^{th} component in the objective function. Different values for λ_is will result in different solutions to the problem. If we want to obtain a smaller leakage interference, we will set a larger λ_1 for the first objective function. If we want to obtain a larger beamforming gain, we will set a larger λ_2 for the second objective function. We will evaluate the performance under different values of λ_is in Section V.

B. SDP formulation

Although we have transformed Problem (14) into Problem (16), it is still hard to solve because of the non-convex constraints. To make the problem tractable, we transform the problem into an SDP through some algebraic transformation. For the objective function, we have

$$
\begin{aligned}
&\lambda_1 \boldsymbol{w}_i^H \tilde{\mathbf{V}}_i^{(0)} (\tilde{\mathbf{V}}_i^{(0)})^H \boldsymbol{w}_i + \lambda_2 \boldsymbol{w}_i^H \mathbf{A}_i \mathbf{A}_i^H \boldsymbol{w}_i \\
&= \mathrm{Tr}(\boldsymbol{w}_i^H (\lambda_1 \tilde{\mathbf{V}}_i^{(0)} (\tilde{\mathbf{V}}_i^{(0)})^H + \lambda_2 \mathbf{A}_i \mathbf{A}_i^H) \boldsymbol{w}_i) \\
&= \mathrm{Tr}((\lambda_1 \tilde{\mathbf{V}}_i^{(0)} (\tilde{\mathbf{V}}_i^{(0)})^H + \lambda_2 \mathbf{A}_i \mathbf{A}_i^H) \boldsymbol{w}_i \boldsymbol{w}_i^H).
\end{aligned} \tag{17}
$$

We denote $\boldsymbol{w}_i \boldsymbol{w}_i^H$ as $\mathbf{W}$. Matrix $\mathbf{W}$ is a symmetric semi-definite matrix with rank one.

The constant-magnitude constraints of Problem (16) are transformed into

$$
\mathbf{W}_{ii} = \frac{1}{N_t}, \ \forall i = 1, ..., N_t, \tag{18}
$$

where $\mathbf{W}_{ii}$ represents the i^{th} diagonal element in $\mathbf{W}$.

Then, Problem (17) is transformed into an SDP as follows:

$$
\begin{aligned}
&SDP(\mathbf{W}^{opt}) = \mathrm{argmax}\{\mathrm{Tr}((\lambda_1 \tilde{\mathbf{V}}_i^{(0)} (\tilde{\mathbf{V}}_i^{(0)})^H + \lambda_2 \mathbf{A}_i \mathbf{A}_i^H) \mathbf{W})\} \\
s.t. \quad &\mathbf{W}_{ii} = \frac{1}{N_t}, \ \forall i = 1, ..., N_t; \\
&\mathbf{W} \succeq 0; \\
&\mathrm{Rank}(\mathbf{W}) = 1.
\end{aligned} \tag{19}
$$

The rank-one constraint is still hard to deal with. In order to efficiently solve the optimization problem, we introduce semidefinite programming relaxation (SDR) by dropping the rank-one constraint in (19) to solve the optimization problem as (20) shows.

$$
\begin{aligned}
&SDR(\mathbf{W}^{opt}) = \mathrm{argmax}\{\mathrm{Tr}((\lambda_1 \tilde{\mathbf{V}}_i^{(0)} (\tilde{\mathbf{V}}_i^{(0)})^H + \lambda_2 \mathbf{A}_i \mathbf{A}_i^H) \mathbf{W})\} \\
s.t. \quad &\mathbf{W}_{ii} = \frac{1}{N_t}, \ \forall i = 1, ..., N_t; \\
&\mathbf{W} \succeq 0.
\end{aligned} \tag{20}
$$

Problem (20) is the relaxed version of Problem (19). Its solution will be an upper bound for the solution of the optimization problem in Problem (19).

C. Approximation

Problem (20) is a standard SDP. Its optimal solution $SDR(\mathbf{W}^{opt})$ can be found by standard tools of mathematical programming such as CVX [38]. Note that Problem (20) is the relaxed version of Problem (19), which means we cannot guarantee $SDR(\mathbf{W}^{opt})$ is rank-one. In fact, according to our simulation results, $SDR(\mathbf{W}^{opt})$ is not necessarily rank-one. When the rank of $SDR(\mathbf{W}^{opt})$ is larger than one, we cannot recover $\boldsymbol{w}_i^{opt}$ from $SDR(\mathbf{W}^{opt})$ straightforwardly. In [39], a randomization technique is used to make an approximation. Its basic idea is to generate a set of candidate vectors $\{\boldsymbol{z}_m\}_{m=1}^{M}$ based on $SDR(\mathbf{W}^{opt})$ and choose the best candidate as the approximation of the $\boldsymbol{w}_i^{opt}$, where M is the size of the set of the candidate vectors.

To be specific, we first generate a set of complex Gaussian vectors $\mathcal{X} = \{\boldsymbol{x}_m \in \mathbb{C}^{N_t \times 1}\}_{m=1}^{M}$. For each $\boldsymbol{x}_m \in \mathcal{X}$, we generate the vector randomly using the distribution $\mathcal{N}(\mathbf{0}, SDR(\mathbf{W}^{opt}))$, where $\mathbf{0} \in \mathbb{C}^{N_t \times 1}$ is the mean vector and $SDR(\mathbf{W}^{opt})$ is the covariance matrix of the Gaussian random vector. In this way, we will have $E[\boldsymbol{x}_m \boldsymbol{x}_m^H] = SDR(\mathbf{W}^{opt})$. However, $\boldsymbol{x}_m$ may not have constant magnitudes for every element, thus it may not be a feasible solution for Problems (19) and (20). To deal with this issue, for each $\boldsymbol{x}_m$, we form $\boldsymbol{z_m} \in \mathbb{C}^{N_t \times 1}$ such that

$$z_m^n = \frac{x_m^n}{\sqrt{N_t}|x_m^n|}, \ \forall n = 1, ..., N_t, \tag{21}$$

where z_m^n is the n^{th} element of vector $\boldsymbol{z}_m$ and x_m^n is the n^{th} element of vector $\boldsymbol{x}_m$. In this way, all the generated $\boldsymbol{z}_m$s satisfy the constant-magnitude constraints, and hence are feasible points for Problems (19) and (20). Therefore, we have

$$\mathrm{Tr}((\lambda_1 \tilde{\mathbf{V}}_i^{(0)} (\tilde{\mathbf{V}}_i^{(0)})^H + \lambda_2 \mathbf{A}_i \mathbf{A}_i^H) \boldsymbol{z}_m \boldsymbol{z}_m^H) \leq SDP(\mathbf{W}^{opt}) \leq SDR(\mathbf{W}^{opt}). \tag{22}$$

Since for all $\boldsymbol{z}_m s$, Inequality (22) will hold, this means

$$\mathrm{Tr}((\lambda_1 \tilde{\mathbf{V}}_i^{(0)} (\tilde{\mathbf{V}}_i^{(0)})^H + \lambda_2 \mathbf{A}_i \mathbf{A}_i^H) E[\boldsymbol{z}_m \boldsymbol{z}_m^H]) \leq SDP(\mathbf{W}^{opt}) \leq SDR(\mathbf{W}^{opt}). \tag{23}$$

Based on Inequality (23), we can choose the $\boldsymbol{z}_m$ from the candidate set $\mathcal{Z} = \{\boldsymbol{z}_m\}_{m=1}^{M}$ that maximizes $\boldsymbol{z}_m^H (\lambda_1 \tilde{\mathbf{V}}_i^{(0)} (\tilde{\mathbf{V}}_i^{(0)})^H + \lambda_2 \mathbf{A}_i \mathbf{A}_i^H) \boldsymbol{z}_m$ as the approximation for $\boldsymbol{w}_i^{opt}$.

Up to now, we have proposed a multi-user analog beamforming method based on the precisely estimated AoD. However, due to the limited feedback and imperfect estimation, we can not obtain the accurate AoD for every path, which makes the proposed beamforming scheme unstable. To deal with the uncertainty in the estimation of AoD, we further propose a robust beamforming scheme in the next section.

IV. Robust Beamforming

To design the robust beamforming scheme, we first need to model the estimation errors. For traditional Rayleigh fading channel models, the estimation errors is simply modeled as a matrix consisting of i.i.d. complex Gaussian distributed entries, which is directly added to the presumed channel. However, in the clustered mmWave channel model, the errors cannot be simply modeled as the additive estimation errors, since the estimated angle errors appear in the index of the exponential function in the array response vectors. Therefore, we need to simplify the error model before designing a robust beamforming scheme.

A. Error model

In this section, we will develop an error model for the ULAs with an array response vector in (5). We assume that for the angle θ_l^i of the path l there exists an angle estimation/quantization error $\Delta\theta_l^i$ with mean 0 and variance σ_l^i. A Gaussian distribution $\mathcal{N}(0,\sigma_l^i)$ is a reasonable assumption, although we only use the first and second order statistics and do not need the distribution. Then, the array response vector with error $\Delta\theta_l^i$ can be expressed as

$$\boldsymbol{\alpha}(\theta_l^i+\Delta\theta_l^i)=\frac{1}{\sqrt{N_t}}[1,e^{j\frac{2\pi}{\lambda}d\sin(\theta_l^i+\Delta\theta_l^i)},...,e^{j(N_t-1)\frac{2\pi}{\lambda}d\sin(\theta_l^i+\Delta\theta_l^i)}]^T. \tag{24}$$

To extract the error out of the exponential function in (24), we expand the exponential function using the first-order Taylor expansion. To simplify the expression, we denote $\frac{2\pi}{\lambda}d$ as κ and the equation (24) is expanded as

$$e^{jn\kappa\sin(\theta_l^i+\Delta\theta_l^i)}\approx e^{jn\kappa\sin(\theta_l^i)}+jn\kappa\cos(\theta_l^i)\Delta\theta_l^i e^{jn\kappa\sin(\theta_l^i)},\forall n=0,...,N_t-1. \tag{25}$$

We denoting $e_l^{i,n}$ as $jn\kappa\cos(\theta_l^i)\Delta\theta_l^i e^{jn\kappa(\sin(\theta_l^i)}$, which represents the error for the n^{th} element in the response vector of the l^{th} path of User i. Error $e_l^{i,n}$ can be written as:

$$e_l^{i,n}=jn\kappa\cos(\theta_l^i)\Delta\theta_l^i\cos(n\kappa(\sin(\theta_l^i))-n\kappa\cos(\theta_l^i)\Delta\theta_l^i\sin(n\kappa(\sin(\theta_l^i)),\forall n=0,...,N_t-1. \tag{26}$$

Defining the error vector $\boldsymbol{e}_l^i\triangleq\frac{1}{\sqrt{N_t}}[e_l^{i,0},e_l^{i,1},...,e_l^{i,N_t-1}]^T$ as the error for the l^{th} path of User i, we now simplify the errors in the AoD into an additive random error as

$$\tilde{\boldsymbol{\alpha}}(\theta_l^i)=\boldsymbol{\alpha}(\theta_l^i+\Delta\theta_l^i)\approx\boldsymbol{\alpha}(\theta_l^i)+\boldsymbol{e}_l^i, \tag{27}$$

where we denote $\tilde{\boldsymbol{\alpha}}(\theta_l^i)$ as the imperfect array response vector of the l^{th} path of User i. Based on the mean and the variance of $\Delta\theta_l^i$, we can calculate the statistical characteristic of $\boldsymbol{e}_l^i$. First, we calculate the statistical characteristic of each element $e_l^{i,n}$ in the vector $\boldsymbol{e}_l^i$. Then, we calculate the cross-covariance between different elements (i.e., $e_l^{i,n}$ and $e_l^{i,m}$ where $m \neq n$) so as to calculate the covariance matrix of e_l^i. The mean and variance of each element $e_l^{i,n}$ are calculated by the following Eqs. (28) and (29).

$$\begin{aligned} E[e_l^{i,n}] = E[\Delta\theta_l^i](jn\kappa\cos(\theta_l^i)\cos(n\kappa(\sin(\theta_l^i))- \\ n\kappa\cos(\theta_l^i)\sin(n\kappa(\sin(\theta_l^i)))) = 0, \forall n = 0, ..., N_t - 1. \end{aligned} \tag{28}$$

$$\begin{aligned} D[e_l^{i,n}] &= E[(e_l^{i,n})^* e_l^{i,n}] = E[(n\kappa\cos(\theta_l^i)\Delta\theta_l^i)^2(\cos^2(n\kappa(\sin(\theta_l^i)) + \sin^2(n\kappa(\sin(\theta_l^i)))] \\ &= (n\kappa\cos(\theta_l^i))^2 E[(\Delta\theta_l^i)^2] = (n\kappa\cos(\theta_l^i)\sigma_l^i)^2, \forall n = 0, ..., N_t - 1. \end{aligned} \tag{29}$$

The cross-covariance between $e_l^{i,n}$ and $e_l^{i,m}$ is calculated as

$$E[(e_l^{i,n})^* e_l^{i,m}] = nm\kappa^2\cos^2(\theta_l^i)(\sigma_l^i)^2, \forall m, n \ and \ m \neq n \tag{30}$$

Based on Equations (29) and (30), we can calculate the covariance matrix of $\boldsymbol{e}_l^i$ as

$$\mathbf{C}_l^i = \begin{bmatrix} 0 & 0 & \cdots & 0 \\ 0 & (\kappa\cos(\theta_l^i)\sigma_l^i)^2 & \cdots & (N_t - 1)\kappa^2\cos^2(\theta_l^i)(\sigma_l^i)^2 \\ \vdots & \vdots & \ddots & \vdots \\ 0 & (N_t - 1)\kappa^2\cos^2(\theta_l^i)(\sigma_l^i)^2 & \cdots & (N_t - 1)^2\kappa^2\cos^2(\theta_l^i)(\sigma_l^i)^2 \end{bmatrix}. \tag{31}$$

Note that the first row and the first column of $\mathbf{C}_l^i$ are all zeros. This is because the first element of the array response vector (24) is always 1, which is independent of an error. In other words, the first element of the array response vector (24) is deterministic and this leads to the zeros in the first row and the first column of $\mathbf{C}_l^i$.

Since we have simplified the AoD error of each path for each user into an additive error, we can further model the errors for the whole AoD matrix as an additive error. Denoting the presumed AoD matrix of User i as $\mathbf{A}_i^p$, the AoD matrix of User i with errors can be modeled as

$$\mathbf{A}_i = \mathbf{A}_i^p + \mathbf{E}_i, \tag{32}$$

where $\mathbf{E}_i = [\boldsymbol{e}_1^i, \boldsymbol{e}_2^i, ..., \boldsymbol{e}_L^i] \in \mathbb{C}^{N_t \times L}$ is a matrix that contains all the error vectors for User i. Based on the assumption that the paths are independent [10] [36], we can assume that the errors of different paths and users are independent, which means

$$E[\boldsymbol{e}_l^i(\boldsymbol{e}_q^i)^H] = \mathbf{0}_{N_t \times N_t}, \quad \forall l \neq q. \tag{33}$$

In (33), $\mathbf{0}_{N_t \times N_t}$ represents the zero square matrix with dimension of N_t. Therefore, the covariance matrix of $\mathbf{E}_i$ is

$$\mathbf{C}_i = \sum_{l=1}^{L_i} \mathbf{C}_l^i. \tag{34}$$

The imperfect leakage interference matrix of User i could also be modeled in the same way as the imperfect AoD matrix. We denote the presumed leakage interference matrix of User i as $\tilde{\mathbf{I}}_i^p = [\mathbf{A}_1^p, ..., \mathbf{A}_{i-1}^p, \mathbf{A}_{i+1}^p, ..., \mathbf{A}_K^p]^T$. The imperfect leakage interference matrix of User i with errors can be modeled as

$$\tilde{\mathbf{I}}_i = \tilde{\mathbf{I}}_i^p + \tilde{\mathbf{E}}_i, \tag{35}$$

where $\tilde{\mathbf{E}}_i = [\mathbf{E}_1, ..., \mathbf{E}_{i-1}, \mathbf{E}_{i+1}, ..., \mathbf{E}_K]^T \in \mathbb{C}^{\sum_{k\neq i}^K L_k \times N_t}$ is a matrix that contains all the error matrices for all the users except User i. We assume the errors of different users are independent, which means

$$E[\mathbf{E}_i \mathbf{E}_j^H] = \mathbf{0}_{N_t \times N_t}, \quad \forall i \neq j. \tag{36}$$

Therefore, the covariance matrix of $\tilde{\mathbf{E}}_i$ is

$$\tilde{\mathbf{C}}_i = \sum_{k\neq i}^{K} \mathbf{C}_k. \tag{37}$$

Now, we have simplified both the errors in the AoD matrix and the leakage interference matrix into the additive error. Based on this error model, we will propose a robust beamforming scheme to confront the uncertainty in the channel information.

B. Robust beamforming

The leakage interference matrix is random due to the uncertainty of errors. This means we cannot find a valid null space of $\tilde{\mathbf{I}}_i$. Therefore, the beamforming method proposed in the previous sections cannot be applied here. To deal with this problem, we use a probabilistic approach to restrict the leakage interference (i.e., we maximize the outage probability). The outage probability can be expressed as

$$P_{outage} = \Pr\{\boldsymbol{w}_i^H \tilde{\mathbf{I}}_i^H \tilde{\mathbf{I}}_i \boldsymbol{w}_i \leq \gamma_i\}, \tag{38}$$

where γ_i denotes a pre-specified leakage power level. Besides the leakage power, we also want to maximize the average beamforming gain of User i, which is defined as

$$BG_{avg} = E[\boldsymbol{w}_i^H \mathbf{A}_i \mathbf{A}_i^H \boldsymbol{w}_i]. \tag{39}$$

We want to maximize the outage probability and the average beamforming gain at the same time. Therefore, a multi-objective optimization problem is constructed as

$$\begin{aligned} \boldsymbol{w}_i^{opt} &= \text{argmax } \{E[\boldsymbol{w}_i^H \mathbf{A}_i \mathbf{A}_i^H \boldsymbol{w}_i], \Pr\{\boldsymbol{w}_i^H \tilde{\mathbf{I}}_i^H \tilde{\mathbf{I}}_i \boldsymbol{w}_i \leq \gamma_i\}\} \\ s.t.\ & \boldsymbol{w}_i \in \mathcal{W}, \end{aligned} \tag{40}$$

where $\mathcal{W}$ is the set of all constant-magnitude vectors with each element having a magnitude of $\frac{1}{\sqrt{N_t}}$. Problem (40) is an MOP with a constant-magnitude constraint and a probabilistic objective function. We first use Markov's inequality to transform the probabilistic objective into the expectation objective. Then, similar to the beamforming scheme we proposed in the previous part, we use the weighted-sum method and the SDP to deal with the multi-objective and constant-magnitude constraint, respectively.

Based on Markov's inequality, we have the following inequality as a foundation for our simplification of the probabilistic objective.

$$\Pr\{Z \leq \gamma\} = 1 - \Pr\{Z \geq \gamma\} \geq 1 - \frac{E[Z]}{\gamma}. \tag{41}$$

Then the probabilistic objective can be simplified as

$$\Pr\{\boldsymbol{w}_i^H \tilde{\mathbf{I}}_i^H \tilde{\mathbf{I}}_i \boldsymbol{w}_i \leq \gamma_i\} = \Pr\{\boldsymbol{w}_i^H (\tilde{\mathbf{I}}_i^p + \tilde{\mathbf{E}}_i)^H (\tilde{\mathbf{I}}_i^p + \tilde{\mathbf{E}}_i) \boldsymbol{w}_i \leq \gamma_i\} \tag{42a}$$

$$\geq 1 - \frac{E[\boldsymbol{w}_i^H (\tilde{\mathbf{I}}_i^p + \tilde{\mathbf{E}}_i)^H (\tilde{\mathbf{I}}_i^p + \tilde{\mathbf{E}}_i) \boldsymbol{w}_i]}{\gamma_i} \tag{42b}$$

$$= 1 - \frac{E[\text{Tr}((\tilde{\mathbf{I}}_i^p + \tilde{\mathbf{E}}_i)^H (\tilde{\mathbf{I}}_i^p + \tilde{\mathbf{E}}_i) \boldsymbol{w}_i \boldsymbol{w}_i^H)]}{\gamma_i} \tag{42c}$$

$$= 1 - \frac{E[\text{Tr}((\tilde{\mathbf{I}}_i^p)^H \tilde{\mathbf{I}}_i^p \boldsymbol{w}_i \boldsymbol{w}_i^H + \tilde{\mathbf{E}}_i^H \tilde{\mathbf{I}}_i^p \boldsymbol{w}_i \boldsymbol{w}_i^H + (\tilde{\mathbf{I}}_i^p)^H \tilde{\mathbf{E}}_i) \boldsymbol{w}_i \boldsymbol{w}_i^H + \tilde{\mathbf{E}}_i^H \tilde{\mathbf{E}}_i \boldsymbol{w}_i \boldsymbol{w}_i^H)]}{\gamma_i} \tag{42d}$$

$$= 1 - \frac{\text{Tr}(E[(\tilde{\mathbf{I}}_i^p)^H \tilde{\mathbf{I}}_i^p \boldsymbol{w}_i \boldsymbol{w}_i^H] + E[\tilde{\mathbf{E}}_i^H \tilde{\mathbf{I}}_i^p] \boldsymbol{w}_i \boldsymbol{w}_i^H + E[(\tilde{\mathbf{I}}_i^p)^H \tilde{\mathbf{E}}_i)] \boldsymbol{w}_i \boldsymbol{w}_i^H + E[\tilde{\mathbf{E}}_i^H \tilde{\mathbf{E}}_i] \boldsymbol{w}_i \boldsymbol{w}_i^H)}{\gamma_i} \tag{42e}$$

$$= 1 - \frac{\text{Tr}(((\tilde{\mathbf{I}}_i^p)^H \tilde{\mathbf{I}}_i^p + \tilde{\mathbf{C}}_i) \boldsymbol{w}_i \boldsymbol{w}_i^H)}{\gamma_i} \tag{42f}$$

$$= 1 - \frac{\text{Tr}(((\tilde{\mathbf{I}}_i^p)^H \tilde{\mathbf{I}}_i^p + \tilde{\mathbf{C}}_i) \mathbf{W})}{\gamma_i}. \tag{42g}$$

In (42e), we exchange the operation order of the expectation and the Tr. Matrix $\mathbf{W} = \boldsymbol{w}_i \boldsymbol{w}_i^H$ is a symmetric semi-definite matrix with rank one. Equations in (42) transform the probabilistic objective function into a deterministic and convex function of $\mathbf{W}$.

The average beamforming gain for User i is an expectation over the instant beamforming gain, which is not easy to deal with. To make the problem tractable, we perform some algebraic transformation and convert it into a deterministic and convex function of $\mathbf{W}$ as below.

$$
\begin{aligned}
& E[\boldsymbol{w}_i^H \mathbf{A}_i \mathbf{A}_i^H \boldsymbol{w}_i] && \text{(43a)}\\
&= E[\boldsymbol{w}_i^H (\mathbf{A}_i^p + \mathbf{E}_i)(\mathbf{A}_i^p + \mathbf{E}_i)^H \boldsymbol{w}_i] && \text{(43b)}\\
&= E[\mathrm{Tr}((\mathbf{A}_i^p + \mathbf{E}_i)(\mathbf{A}_i^p + \mathbf{E}_i)^H \boldsymbol{w}_i \boldsymbol{w}_i^H] && \text{(43c)}\\
&= \mathrm{Tr}(E[(\mathbf{A}_i^p + \mathbf{E}_i)(\mathbf{A}_i^p + \mathbf{E}_i)^H \boldsymbol{w}_i \boldsymbol{w}_i^H]) && \text{(43d)}\\
&= \mathrm{Tr}(E[\mathbf{A}_i^p (\mathbf{A}_i^p)^H \boldsymbol{w}_i \boldsymbol{w}_i^H] + E[\mathbf{E}_i (\mathbf{A}_i^p)^H + \mathbf{A}_i^p \mathbf{E}_i^H] \boldsymbol{w}_i \boldsymbol{w}_i^H + E[\mathbf{E}_i \mathbf{E}_i^H] \boldsymbol{w}_i \boldsymbol{w}_i^H) && \text{(43e)}\\
&= \mathrm{Tr}((\mathbf{A}_i^p (\mathbf{A}_i^p)^H + \mathbf{C}_i) \boldsymbol{w}_i \boldsymbol{w}_i^H) && \text{(43f)}\\
&= \mathrm{Tr}((\mathbf{A}_i^p (\mathbf{A}_i^p)^H + \mathbf{C}_i) \mathbf{W}). && \text{(43g)}
\end{aligned}
$$

The introduction of matrix $\mathbf{W}$ will transform the non-convex constraints on $\boldsymbol{w}_i$ into

$$\mathbf{W}_{ii} = \frac{1}{N_t}, \ \forall i = 1, ..., N_t, \tag{44}$$

where $\mathbf{W}_{ii}$ represents the i^{th} diagonal element in $\mathbf{W}$. This constraints are convex constraints and are easy to deal with.

Based on the above three simplifications, using the weighted-sum method, we can reformulate Problem (40) into

$$
\begin{aligned}
& SDP_{robust}(\mathbf{W}^{opt}) = \mathrm{argmax} \left\{ \lambda_1 \mathrm{Tr}((\mathbf{A}_i^p (\mathbf{A}_i^p)^H + \mathbf{C}_i)\mathbf{W}) + \lambda_2 \left(1 - \frac{\mathrm{Tr}(((\tilde{\mathbf{I}}_i^p)^H \tilde{\mathbf{I}}_i^p + \tilde{\mathbf{C}}_i)\mathbf{W})}{\gamma_i} \right) \right\} \\
s.t. \quad & \mathbf{W}_{ii} = \frac{1}{N_t}, \ \forall i = 1, ..., N_t; \\
& \mathbf{W} \succeq 0; \\
& \mathrm{Rank}(\mathbf{W}) = 1,
\end{aligned} \tag{45}
$$

where $\lambda_1 + \lambda_2 = 1$. Parameter λ_i represents the importance of the i^{th} component in the cost function.

To deal with the rank-one constraint, we introduce the SDR by dropping the rank constraint in (45). Therefore, an upper bound of Problem (45) can be achieved.

$$SDR_{robust}(\mathbf{W}^{opt}) = \mathrm{argmax}\left\{\lambda_1 \,\mathrm{Tr}((\mathbf{A}_i^p(\mathbf{A}_i^p)^H + \mathbf{C}_i)\mathbf{W}) + \lambda_2\left(1 - \frac{\mathrm{Tr}(((\tilde{\mathbf{I}}_i^p)^H\tilde{\mathbf{I}}_i^p + \tilde{\mathbf{C}}_i)\mathbf{W})}{\gamma_i}\right)\right\}$$
$$s.t. \quad \mathbf{W}_{ii} = \frac{1}{N_t}, \ \forall i = 1, ..., N_t;$$
$$\mathbf{W} \succeq 0. \tag{46}$$

The optimal solution $SDR_{robust}(\mathbf{W}^{opt})$ can be found by standard tools of mathematical programming [38]. Using the same approximation method as in the non-robust case, we can obtain the analog beamforming vector $\boldsymbol{w}_i^{opt}$.

V. Simulation Results

In this section, we evaluate the performance of the non-robust beamforming method in Section III and the robust beamforming method in Section IV. Note that our objective in this paper is not to optimize the sum-rate due to the intractability of doing so. In fact, we strike a balance between maximizing the beamforming gain and minimizing the inter-user interference. Since the λ_i represents the importance of each term in the objective function of the MOP, we expect to find the best balance by evaluating different assignments of values of $\lambda_i s$. Therefore, we pick the combination of λ_1 and λ_2 that achieve the highest sum-rate. We also compare our multi-user analog beamforming with the beam selection method and other traditional fully-digital beamforming methods. For the robust beamforming method, we compare our robust analog beamforming with the non-robust ones to evaluate the improvement brought by our method.

A. Non-robust analog beamforming

In the simulation, we consider a multi-user MIMO system consisting of one BS equipped with a large antenna array and K single-antenna users. The channels are realized using Eq. (4). Due to the limited scattering characteristic of the mmWave channels, the number of paths should be small. Here, we assume each channel has $L = 6$ paths. The large antenna array at the BS is assumed to have $N_t = 64$ antennas, which is the same number of antennas in [40]. To leave enough dimension for the null space of the leakage interference, we assume the total number of users $K = 6$. This will leave $N_t - KL = 28$ dimensions for the null space. The θ_l^i of each path is assumed to be uniformly distributed in $[0, 2\pi]$. The results are averaged over $20,000$ channel realizations. The variance of AWGN noise per user is assumed to be the same for all users, i.e. $\sigma_1^2 = ... = \sigma_K^2 = \sigma^2$. And the large-scale fading path loss factor of all users are uniformly distributed in $[0.5, 1.5]$ dB. We have used these parameters in all figures unless we specifically mention otherwise.

Figs. 2 and 3 illustrate the sum-rate and the beamforming gain and interference of our analog beamforming under different λ_1 and λ_2 values, respectively. We, in general, evaluate 21 combinations of λ_1 and λ_2. To be specific, the λ_2 ranges from 0 to 1 with step-size 0.05 and $\lambda_1 = 1 - \lambda_2$. In Fig. 2, as λ_2 increases from 0 to 1, the sum-rate first increases and then decreases, which exhibits the tradeoff between the beamforming gain and the leakage interference. In Fig. 3, when $\lambda_2 = 0$, the leakage interference is minimized but the beamforming gain is quite low. When $\lambda_1 = 1$, the beamforming gain is maximized but the leakage interference is very high. Fig. 2 shows that there is a tradeoff between leakage interference and beamforming gain and as a result the MOP provides better performance than only optimizing beamforming gain or interference. Note that there is no need to set different weights for different users because we deal with a decoupled problem, i.e., the best λ_2 for each user should be the same. For example, when we fix the parameters for other users and change the weight the for User 1, the trend in the plot should be similar to Fig. 2. Therefore, we will set $\lambda_1 = 0.9$ and $\lambda_2 = 0.1$, which achieves the best sum-rate, for all users in the follow-up simulations.

To further illustrate the relationship between the two objectives in Problem (14), we plot Fig. 4 to show the tradeoff between beamforming gain and the norm of the projection of $\boldsymbol{w}_i$ onto the null space. As the beamforming gain increases, the norm of the projection decreases. As such, the use of multiple-objective optimization is justified.

In Fig. 5, the proposed analog non-robust beamforming method is compared with the analog beam selection method in [24], the digital ZF beamforming [4], [17] and the digital SLNR beamforming [13], [14], [16]. The analog beam selection method usually needs a hierarchical search to find the best beam, which results in a high training overhead. In our simulation, for simplicity, we directly use the array response vector of the strongest path of each user, which is the best beam for each user, as the solution for the analog beam selection. This is equivalent to a codebook with infinite vectors. As such, the performance of the beam selection that we report is better than what presented in [24]–[26]. Fig. 5 shows the empirical cumulative distribution function (CDF) of SINR when the $SNR = 25dB$ for different methods. For a fixed

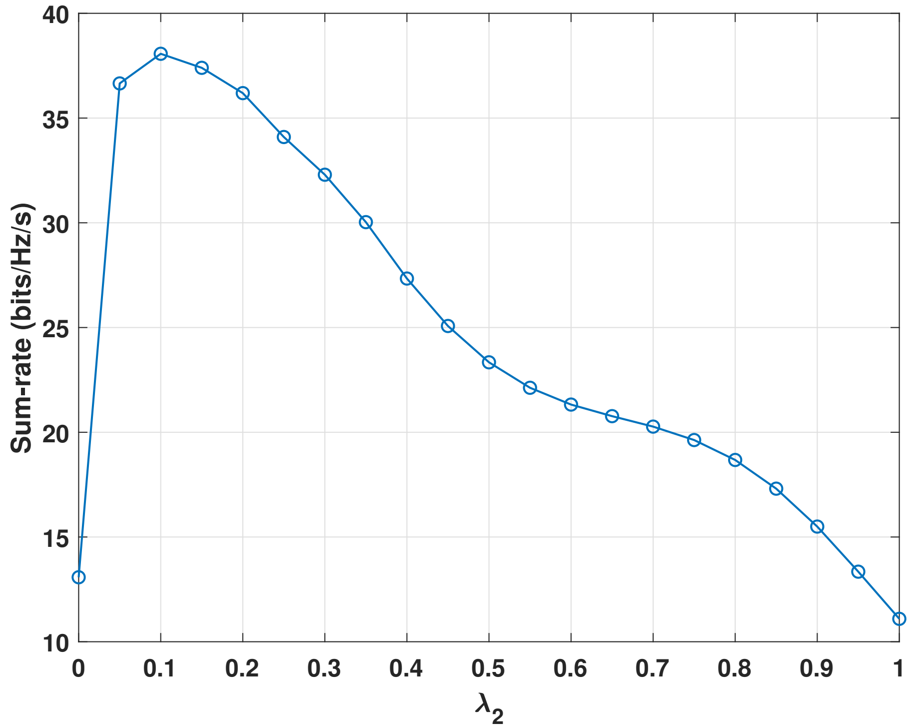

Fig. 2: Sum-rate evaluation for different combinations of sum weights

SINR value a, the corresponding CDF value p implies that $Pr(SINR \leq a) = p$. At $SINR = 0dB$, the corresponding CDFs of the digital SLNR beamformer, the digital ZF beamformer, our proposed analog ZF beamformer, and the beam selection method are around 0%, 2%, 2%, and 10%, respectively. At $SINR = 15dB$, the CDF numbers are around 0%, 10%, 30%, and 75%, respectively. Generally speaking, the fully digital beamformers have CDF values that are lower than those of the analog beamformers at every SINR while requiring a higher cost of RF chains. Note that, the fully digital beamforming methods such as the zero-forcing method and the SLNR-based method are only used as the benchmark. The analog beamforming cannot outperform the fully digital beamforming. Besides, we only use the channel phase information, which will lead to performance degradation. The main method we are comparing with is the beam selection method, which is the main analog beamforming method adopted in mmWave systems and our proposed method has a much lower CDF value at most SINRs compared to the beam selection method. This is because we suppress the interference in our model while the beam selection method only maximizes the beamforming gain.

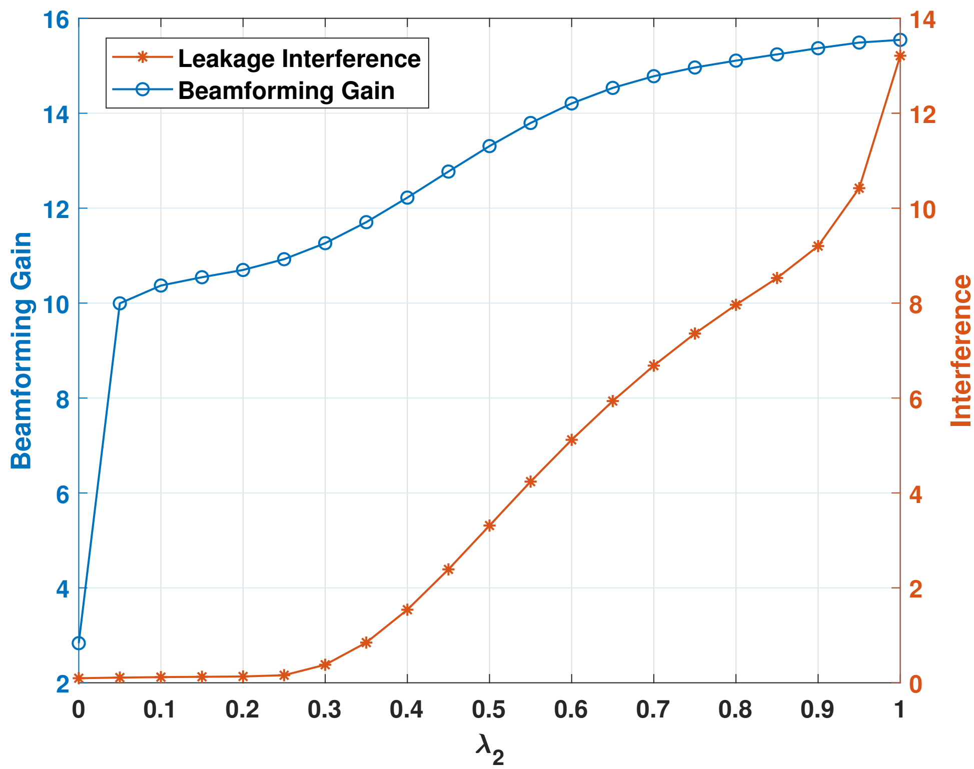

Fig. 3: Beamforming Gain and Interference for different combinations of sum weights

To have an overall observation of the performance of the three methods, we plot the average sum-rate per user with SNR ranging from -15 dB to 30 dB in Fig. 6. The fully digital SLNR-based beamforming method has the best performance at every SNR. When the SNR is low, the beam selection method performs better compared to both the digital ZF beamformer and the proposed analog beamformer. For example, when SNR is 0 dB, the sum-rate of the beam selection is around 10, while the sum-rates of our proposed analog beamformer and the digital ZF beamformer are around 6 and 5, respectively. Although our proposed analog beamformer cannot beat the beam selection method at low SNR, it performs better than the digital ZF beamformer. The reason why our proposed analog beamformer cannot beat the beam selection method when SNR is low is because we only use partial channel information (AoD matrix), not the entire channel in (4), to maximize the beamforming gain. When the SNR is low, the power of interference can be ignored because the noise power is large, therefore, the method with the largest beamforming gain will have the largest SINR thus the best sum-rate. Note that, in our simulations, we directly use the array response vector of the strongest path as the beam selected

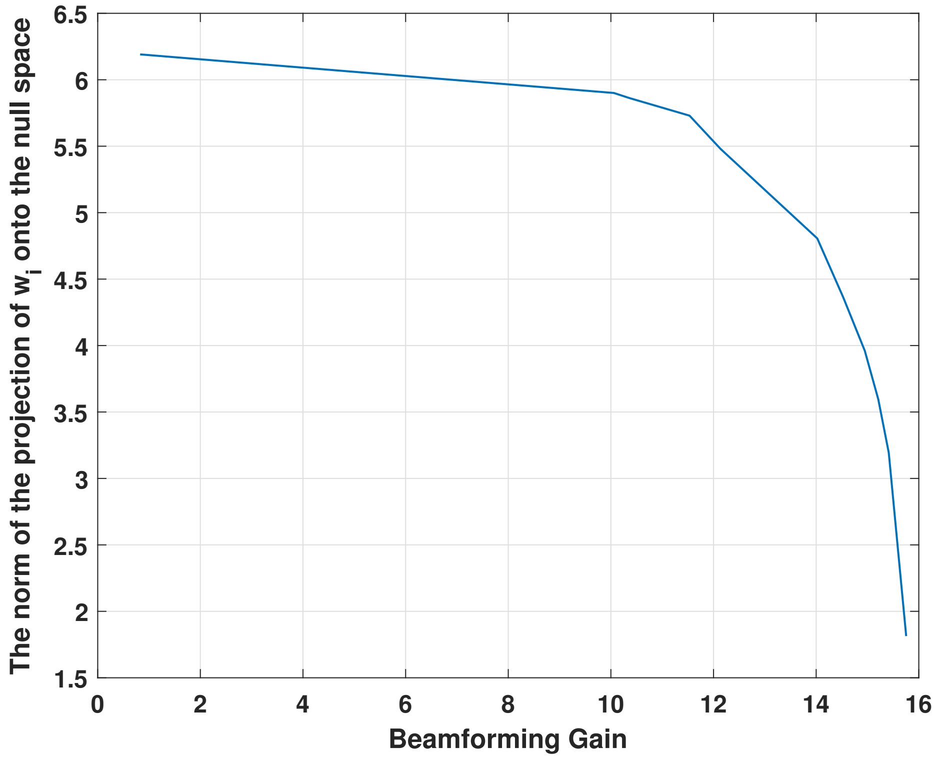

Fig. 4: The tradeoff between the beamformining gain and the norm of the projection of $\boldsymbol{w}_i$ onto the null space

for User i, which is the best performance for the beam selection, without considering any beam alignment loss. Therefore, as mentioned before, the beam selection method in our simulations would perform better than what presented in [24]–[26]. However, when the SNR is large, for example 25 dB, the performance of the beam selection is the worst among the four methods due to the severe interference. When the SNR is 25 dB, our proposed analog beamformer can achieve a sum-rate of about 35 while the sum-rate of the beam selection only reaches 21.

Although the beam selection method has a better performance in the low SNR region, it needs a multi-stage training process to obtain the precise beam, which will result in a waste of transmission resources. Our method, on the other hand, only needs one-stage feedback of the AoD, thus saving transmission resources. Moreover, to increase the precision of the beam direction for the beam selection method, one should increase the training overhead. However, we have proposed a robust beamforming method to confront the estimation/quantization error in the AoD. Our robust beamforming method can further reduce the feedback overhead since

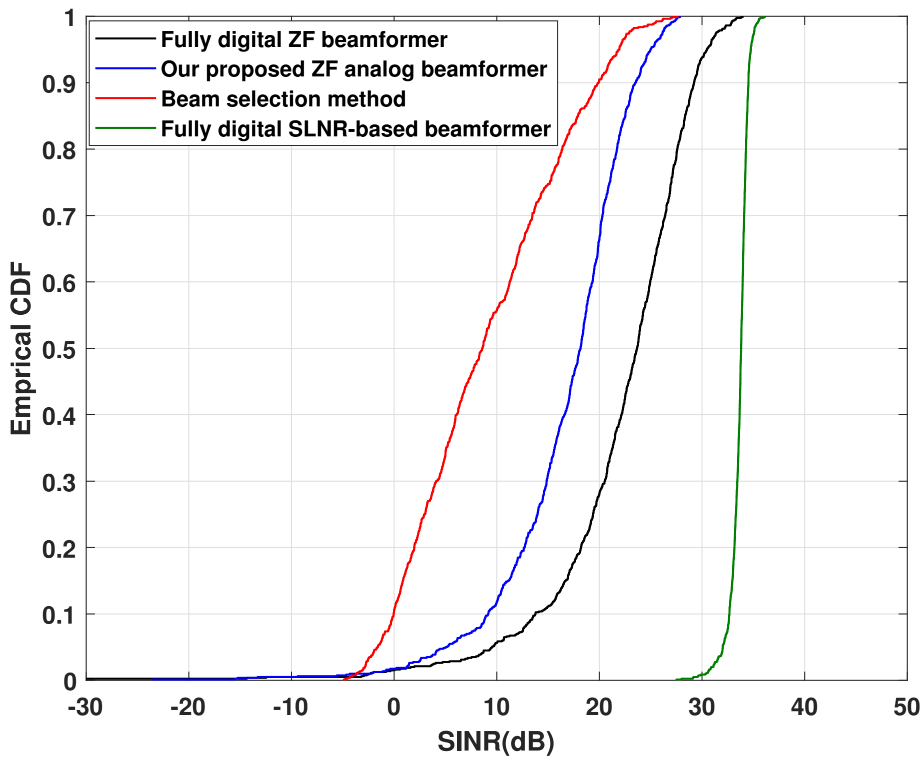

Fig. 5: CDF of SINR when SNR=25dB

we do not need to know a completely precise AoD as confirmed by the simulations in the next section.

B. Robust analog beamforming

For the robust case, we evaluate the sum-rate performance with different levels of uncertainty, i.e. the error variance $\sigma_{error}^2 = \{0.005, 0\}$. The leakage power level is set to be $\gamma_i = 0.1, \forall i = 1, \ldots, K$. We compare the performance of the proposed robust analog beamfomer, the non-robust digital ZF beamformer, the beam selection method, and the non-robust digital SLNR-based beamformer. In the previous section, we assumed an infinite codebook for the beam selection method, which avoids the quantization error. In this section, for the beam selection method, we assume there exists an error in the beam alignment angle and this error has the same statistical characteristic as the error in AoDs.

When the error variance $\sigma_{error}^2 = 0$, we will have the same results as in the non-robust case. In fact, the ideas behind these two beamformers are the same. For the robust beamformer, when

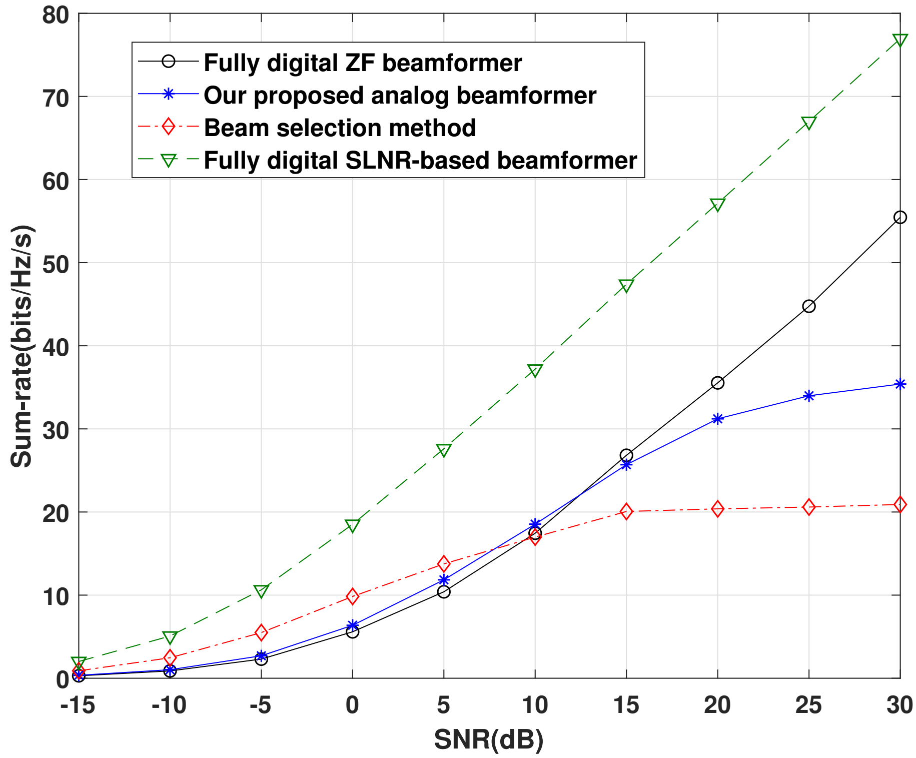

Fig. 6: Sum-rate comparison

the error variance is 0, we actually minimize $\text{Tr}((\tilde{\mathbf{I}}_i^p)^H \tilde{\mathbf{I}}_i^p \mathbf{W})$, i.e., the leakage power of User i. This is the same as maximizing the projection of $\boldsymbol{w}_i$ onto the null space of $\tilde{\mathbf{I}}_i^p$, which is what we do for the non-robust beamformer.

Fig. 7 shows the SINR CDF of the three beamforming approaches when $\sigma_{error}^2 = 0.005$. We set the $SNR = 25dB$. The proposed analog beamformer has a large improvement in performance compared with the beam selection method and the non-robust ZF beamformer. For example, when $SINR = 0dB$, the CDF values of the proposed robust analog beamformer, the beam selection method, the non-robust digital ZF beamformer and the non-robust SLNR-based beamformer are around 15%, 52%, 58% and 61%, respectively. When CDF is at 50%, the proposed robust analog beamformer can provide 11 dB ,12 dB and 13 dB improvement in SINR compared with the beam selection method, the non-robust ZF beamformer and the non-robust SLNR-based beamformer, respectively.

Fig. 8 plots the averaged sum-rate per user of the three beamforming methods when the SNR ranges from -15dB to 30dB with $\sigma_{error}^2 = 0.005$. The proposed robust analog beamformer

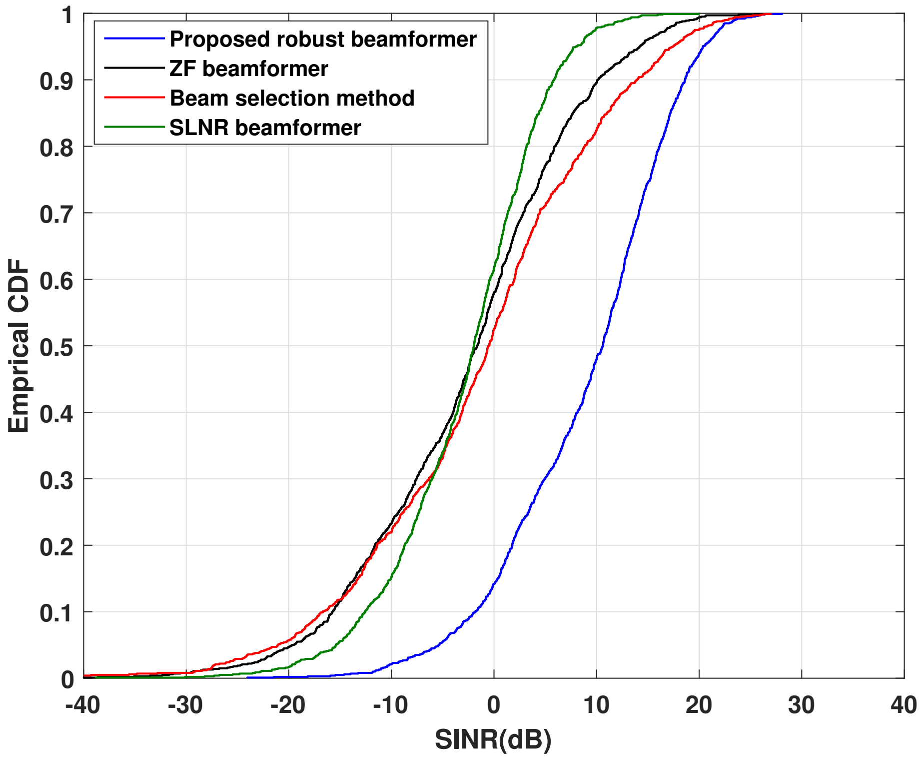

Fig. 7: CDF of SINR when SNR=25dB. The variance of error is 0.005

outperforms both the beam selection method and the non-robust ZF beamformer at every SNR. When SNR is 25dB, the proposed beamformer provides an improvement of 109%, 188% and 254% of the averaged sum-rate with respect to that of the beam selection method, the non-robust ZF beamformer and the non-robust SLNR-based beamformer, respectively.

Both Figs. 7 and 8 show that a slight estimation error will lead to severe system performance degradation. However, and our robust beamforming scheme can provide large improvement for imperfect CSI scenarios.

VI. Conclusion

In this paper, we proposed an analog beamforming scheme which strikes a balance between the beamforming gain and the inter-user interference. We formulated an MOP that maximizes the beamforming gain and minimizes the interference at the same time. The weighted-sum method was used to transform the MOP into an SOP and the SDP was adopted to make the constant-magnitude constraints for the analog beamforming tractable. Furthermore, to alleviate

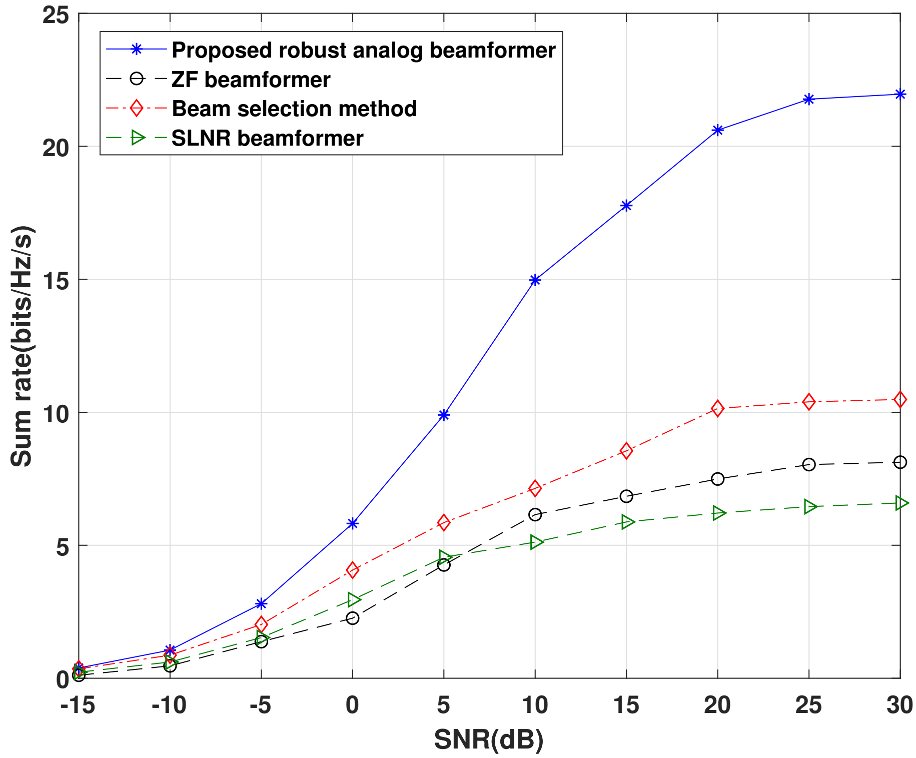

Fig. 8: Averaged sum-rate per user. The variance of error is 0.005

the effects of the channel estimation and feedback quantization errors, we designed a robust beamforming scheme to overcome the channel uncertainty. A probabilistic constraint was used and an MOP similar with the non-robust beamforming scheme was formulated. For the non-robust case, simulation results showed that the proposed beamformer provides a better balance between the beamforming gain and the inter-user interference compared with other analog beamformers in the high SNR region. For the robust case, the simulation results demonstrated the highest robustness of our beamforming scheme against channel errors.

REFERENCES

[1] T. S. Rappaport, R. W. Heath Jr, R. C. Daniels, and J. N. Murdock, *Millimeter wave wireless communications*. Pearson Education, Sep. 2014.

[2] E. Torkildson, B. Ananthasubramaniam, U. Madhow, and M. Rodwell, "Millimeter-wave MIMO: Wireless links at optical speeds," in *Proc. of 44th Allerton Conference on Communication, Control and Computing*, Monticello, Illinois, USA, Sep. 2006.

[3] J. N. Murdock, E. Ben-Dor, Y. Qiao, J. I. Tamir, and T. S. Rappaport, "A 38 GHz cellular outage study for an urban

outdoor campus environment," in *Proc. of 2012 IEEE Wireless Communications and Networking Conference (WCNC)*, Paris, France, Apr. 2012.

[4] H. Jafarkhani, *Space-time coding: theory and practice*. Cambridge university press, Sep. 2005.

[5] A. Goldsmith, *Wireless communications*. Cambridge university press, Aug. 2005.

[6] D. Tse and P. Viswanath, *Fundamentals of wireless communication*. Cambridge university press, May. 2005.

[7] L. Liu and H. Jafarkhani, "Space-time trellis codes based on channel-phase feedback," *IEEE Transactions on Communications*, vol. 54, no. 12, pp. 2186–2198, Dec. 2006.

[8] A. Hottinen, O. Tirkkonen, and R. Wichman, *Multi-antenna transceiver techniques for 3G and beyond*. John Wiley & Sons, Aug. 2004.

[9] A. Narula, M. J. Lopez, M. D. Trott, and G. W. Wornell, "Efficient use of side information in multiple-antenna data transmission over fading channels," *IEEE Journal on Selected Areas in Communications*, vol. 16, no. 8, pp. 1423–1436, Oct. 1998.

[10] O. El Ayach, S. Rajagopal, S. AbuSurra, Z. Pi, and R. W. Heath, "Spatially sparse precoding in millimeter wave MIMO systems," *IEEE Transactions on Wireless Communications*, vol. 13, no. 3, pp. 1499–1513, Mar. 2014.

[11] K. Wong, R. Cheng, K. B. Letaief, and R. D. Murch, "Adaptive antennas at the mobile and base stations in an OFDM/TDMA system," *IEEE Transactions on Communications*, vol. 49, no. 1, pp. 195–206, Jan. 2001.

[12] M. Schubert and H. Boche, "Solution of the multiuser downlink beamforming problem with individual SINR constraints," *IEEE Transactions on Vehicular Technology*, vol. 53, no. 1, pp. 18–28, Jan. 2004.

[13] A. Tarighat, M. Sadek, and A. H. Sayed, "A multi user beamforming scheme for downlink MIMO channels based on maximizing signal-to-leakage ratios," in *Proc. of IEEE International Conference on Acoustics, Speech, and Signal Processing Proceedings (ICASSP'05)*, Philadelphia, Pennsylvania, USA, Mar. 2005.

[14] M. Sadek, A. Tarighat, and A. H. Sayed, "Active antenna selection in multiuser MIMO communications," *IEEE Transactions on Signal Processing*, vol. 55, no. 4, pp. 1498–1510, Apr. 2007.

[15] A. Wiesel, Y. C. Eldar, and S. Shamai, "Linear precoding via conic optimization for fixed MIMO receivers," *IEEE Transactions on Signal Processing*, vol. 54, no. 1, pp. 161–176, Jan. 2006.

[16] L. C. Godara, *Handbook of antennas in wireless communications*. CRC press, Aug. 2001.

[17] Q. H. Spencer, A. L. Swindlehurst, and M. Haardt, "Zero-forcing methods for downlink spatial multiplexing in multiuser MIMO channels," *IEEE Transactions on Signal Processing*, vol. 52, no. 2, pp. 461–471, Feb. 2004.

[18] A. Alkhateeb, G. Leus, and R. W. Heath, "Limited feedback hybrid precoding for multi-user millimeter wave systems," *IEEE Transactions on Wireless Communications*, vol. 14, no. 11, pp. 6481–6494, Nov. 2015.

[19] W. Ni and X. Dong, "Hybrid block diagonalization for massive multiuser MIMO systems," *IEEE Transactions on Communications*, vol. 64, no. 1, pp. 201–211, Jan. 2016.

[20] R. Rajashekar and L. Hanzo, "Iterative matrix decomposition aided block diagonalization for mm-wave multiuser MIMO systems," *IEEE Transactions on Wireless Communications*, vol. 16, no. 3, pp. 1372–1384, Mar. 2017.

[21] X. Li, Y. Zhu, and P. Xia, "Enhanced analog beamforming for single carrier millimeter wave MIMO systems," *IEEE Transactions on Wireless Communications*, vol. 16, no. 7, pp. 4261–4274, Jul. 2017.

[22] H. Lee and Y. Ko, "Non-iterative symbol-wise beamforming for MIMO-OFDM systems," *IEEE Transactions on Wireless Communications*, vol. 11, no. 10, pp. 3788–3798, Oct. 2012.

[23] A. Pollok, W. G. Cowley, and N. Letzepis, "Symbol-wise beamforming for MIMO-OFDM transceivers in the presence of co-channel interference and spatial correlation," *IEEE Transactions on Wireless Communications*, vol. 8, no. 12, pp. 5755–5760, Dec. 2009.

[24] J. Wang, "Beam codebook based beamforming protocol for multi-Gbps millimeter-wave WPAN systems," *IEEE Journal on Selected Areas in Communications*, vol. 27, no. 8, pp. 1390–1399, Oct. 2009.

[25] Y. M. Tsang, A. S. Poon, and S. Addepalli, "Coding the beams: Improving beamforming training in mmWave communication system," in *Proc. of 2011 IEEE Global Telecommunications Conference (GLOBECOM 2011)*, Houston, Texas, USA, Dec. 2011.

[26] S. Hur, T. Kim, D. J. Love, J. V. Krogmeier, T. A. Thomas, and A. Ghosh, "Millimeter wave beamforming for wireless backhaul and access in small cell networks," *IEEE Transactions on Communications*, vol. 61, no. 10, pp. 4391–4403, Oct. 2013.

[27] S. Ekbatani, F. Etemadi, and H. Jafarkhani, "Throughput maximization over slowly fading channels using quantized and erroneous feedback," *IEEE Transactions on Communications*, vol. 57, no. 9, pp. 2528–2533, Sep. 2009.

[28] S. Ekbatani and H. Jafarkhani, "Combining beamforming and space-time coding using noisy quantized feedback," *IEEE Transactions on Communications*, vol. 57, no. 5, pp. 1280–1286, May. 2009.

[29] S. Ekbatani, F. Etemadi, and H. Jafarkhani, "Outage behavior of slow fading channels with power control using partial and erroneous csit," *IEEE Transactions on Information Theory*, vol. 56, no. 12, pp. 6097–6102, Dec. 2010.

[30] H. Du and P. Chung, "A probabilistic approach for robust leakage-based MU-MIMO downlink beamforming with imperfect channel state information," *IEEE Transactions on Wireless Communications*, vol. 11, no. 3, pp. 1239–1247, Mar. 2012.

[31] B. K. Chalise, S. Shahbazpanahi, A. Czylwik, and A. B. Gershman, "Robust downlink beamforming based on outage probability specifications," *IEEE Transactions on Wireless Communications*, vol. 6, no. 10, pp. 3498–3503, Oct. 2007.

[32] P. Chung, H. Du, and J. Gondzio, "A probabilistic constraint approach for robust transmit beamforming with imperfect channel information," *IEEE Transactions on Signal Processing*, vol. 59, no. 6, pp. 2773–2782, Jun. 2011.

[33] L. Liu, Y. Nam, and J. Zhang, "Proportional fair scheduling for multi-cell multi-user mimo systems," in *Proc. of IEEE 44th Annual Conference on Information Sciences and Systems (CISS)*, Princeton, New Jersey, USA, Mar. 2010.

[34] J. Kazemitabar and H. Jafarkhani, "Multiuser interference cancellation and detection for users with more than two transmit antennas," *IEEE Transactions on Communications*, vol. 56, no. 4, pp. 574–583, Apr. 2008.

[35] T. S. Rappaport, F. Gutierrez, E. BenDor, J. N. Murdock, Y. Qiao, and J. I. Tamir, "Broadband millimeter-wave propagation measurements and models using adaptive-beam antennas for outdoor urban cellular communications," *IEEE Transactions on Antennas and Propagation*, vol. 61, no. 4, pp. 1850–1859, Apr. 2013.

[36] O. El Ayach, R. W. Heath, S. AbuSurra, S. Rajagopal, and Z. Pi, "The capacity optimality of beam steering in large millimeter wave MIMO systems," in *Proc. of IEEE 13th International Workshop on Signal Processing Advances in Wireless Communications (SPAWC)*, Cesme, Turkey, Jun. 2012.

[37] R. T. Marler and J. S. Arora, "The weighted sum method for multi-objective optimization: new insights," *Structural and Multidisciplinary Optimization*, vol. 41, no. 6, pp. 853–862, Jun. 2010.

[38] M. Grant, S. Boyd, and Y. Ye, "CVX: Matlab software for disciplined convex programming," 2008.

[39] I. Waldspurger, A. d'Aspremont, and S. Mallat, "Phase recovery, maxcut and complex semidefinite programming," *Mathematical Programming*, vol. 149, no. 1-2, pp. 47–81, Feb. 2015.

[40] "New SID proposal: Study on full dimension MIMO for LTE," 3GPP TSG RAN Meeting 58, Tech. Rep., Dec. 2012.